

# Aortic annulus sizing using watershed transform and morphological approach for CT images

Cite as: AIP Conference Proceedings 1930, 020048 (2018); <https://doi.org/10.1063/1.5022942>  
Published Online: 02 February 2018

Norhasmira Mohammad, Zaid Omar and Mus'ab Sahrim



View Online



Export Citation

## ARTICLES YOU MAY BE INTERESTED IN

[The effect of sodium hydroxide on drag reduction using banana peel as a drag reduction agent](#)

AIP Conference Proceedings 1930, 020031 (2018); <https://doi.org/10.1063/1.5022925>

[Rice husk ash \(RHA\) as a partial cement replacement in modifying peat soil properties](#)

AIP Conference Proceedings 1930, 020046 (2018); <https://doi.org/10.1063/1.5022940>

[Full cycle trigonometric function on Intel Quartus II Verilog](#)

AIP Conference Proceedings 1930, 020044 (2018); <https://doi.org/10.1063/1.5022938>

1.8 GHz

8.5 GHz

**Trailblazers.** New

Meet the Lock-in Amplifiers that measure microwaves.

Zurich Instruments

Find out more

# Aortic Annulus Sizing Using Watershed Transform and Morphological Approach for CT Images

Norhasmira Mohammad<sup>1, a)</sup>, Zaid Omar<sup>2, b)</sup> and Mus'ab Sahrin<sup>3, c)</sup>

<sup>1</sup>*Faculty of Biosciences and Medical Engineering, Universiti Teknologi Malaysia, 81310 Skudai, Johor, Malaysia*

<sup>2</sup>*Faculty of Electrical Engineering, Universiti Teknologi Malaysia, 81310 Skudai, Johor, Malaysia*

<sup>3</sup>*Faculty of Engineering and Built Environment, Universiti Sains Islam Malaysia, 71800 Nilai, Negeri Sembilan, Malaysia*

<sup>b)</sup>Corresponding author: zaidomar@utm.my

<sup>a)</sup>norhasmira.mohammad@gmail.com

<sup>c)</sup>musab@usim.edu.my

**Abstract.** Aortic valve disease occurs due to calcification deposits on the area of leaflets within the human heart. It is progressive over time where it can affect the mechanism of the heart valve. To avoid the risk of surgery for vulnerable patients especially senior citizens, a new method has been introduced: Transcatheter Aortic Valve Implantation (TAVI), which places a synthetic catheter within the patient's valve. This entails a procedure of aortic annulus sizing, which requires manual measurement of the scanned images acquired from Computed Tomographic (CT) by experts. The step requires intensive efforts, though human error may still eventually lead to false measurement. In this research, image processing techniques are implemented onto cardiac CT images to achieve an automated and accurate measurement of the heart annulus. The image is first put through pre-processing for noise filtration and image enhancement. Then, a marker image is computed using the combination of opening and closing operations where the foreground image is marked as a feature while the background image is set to zero. Marker image is used to control the watershed transformation and also to prevent oversegmentation. This transformation has the advantage of fast computational and oversegmentation problems, which usually appear with the watershed transform can be solved with the introduction of marker image. Finally, the measurement of aortic annulus from the image data is obtained through morphological operations. Results affirm the approach's ability to achieve accurate annulus measurements compared to conventional techniques.

## INTRODUCTION

Aortic Stenosis (AS) is also known as heart valve disease which requires an open heart surgery to treat the patient. Traditionally, patient who suffers from heart valve calcification will undergo the surgical aortic valve replacement (SAVR). However, the risk of the procedure is high. Transcatheter aortic valve implantation (TAVI) technique has proved to be a realistic alternative therapy to SAVR [1]. It is a less invasive procedure for patients with severe, symptomatic aortic stenosis who are otherwise left untreated due to the perceived high risk of operative mortality [2]. Procedure involves in inserting a new artificial heart valve inside the old valve that is severely calcified using balloon catheter. The selection of patients is based on the risk score of the Society of Thoracic Surgeons -Predicted of Mortality score (STS-PROM) and the European System for Cardiac Operative Risk Evaluation (EuroScore) [3-5]. TAVI procedure requires the patient to first undergo the pre-TAVI assessment to determine the exact size of the prosthetic valve where cardiac image acquire form CT scan is needed. Figure 1 shows the example of region of interest (ROI) in CT scan image which include the area of ascending aorta (AA) and left ventricular outflow tract (LVOT). The black arrow represents the size of annulus.

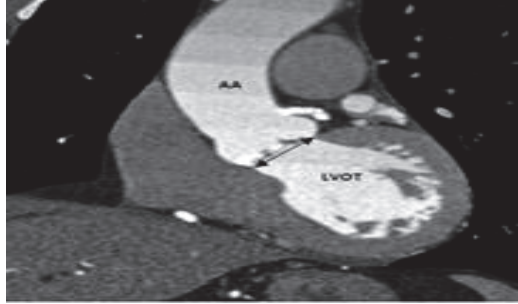


**FIGURE 1.** Aortic valve in CT image

## **IMAGE PROCESSING ON MEDICAL IMAGE**

Image segmentation is the process of preserving the interest objects in the image from the background, dividing the image into separate regions such that each region is homogeneous with respect to some properties such as grey value or texture [6]. There are several common approaches to segmentation which are thresholding, edge-based segmentation and region-based segmentation. Thresholding is a method of separating the light and dark regions in the image. It creates binary images from grey-level ones by turning all pixels below some threshold to zero and all pixels about that threshold to one [7].

In edge-based segmentation, the algorithm detects and links the edge pixels to form contours. Two steps are needed in this method; edge detection and edge linking. The edges are detected using several gradient operators such as canny, LoG and Laplacian while edge linking requires magnitude of the gradient and the direction of gradient vector. Then, edges in a predefined neighborhood are linked if both magnitude and direction criteria are satisfied [7].

Finally, region-based segmentation algorithms operate iteratively by grouping together pixels, which are neighbours and have similar values and splitting groups of pixels which are dissimilar in value [7]. Watershed transform is one of the examples of region-based methods for segmentation and it is proven to produce good segmentation results and the basic operation of segmentation is based on mathematical morphology [8]. In [9], they provided a good explanation on watershed transform associated the sequential algorithm. They also introduced the needs of distinguishing between definition, algorithm specification and algorithm implementation in their study. Various examples are given which illustrated differences between watershed transforms based on different definitions and implementations. The second part of the paper discussed about parallel implementation of sequential watershed algorithms.

In a meantime, combinations of watershed transform with other processing method also produce convenient results. As in [10], they combined a watershed transform and probabilistic atlas to perform segmentation. The basic idea of the method presented in this paper is reflected in the combined application of two techniques: a-prior knowledge derived from a density based probabilistic atlas is used to locate characteristic parts of the object and a watershed transform to identify spatially coherent sub-volumes, regardless of their density. The fundamental idea of the proposed method of tissue classification using information in both the spatial domain and the density domain is reflected in the combined use of density based spatial information and shape based information obtained from a watershed transform.

Other than that, interactive watershed transform (IWT) has been successfully applied to a large variety of medical images, for instance in segmentation and volumetric of neuroanatomic structures as well as bone segmentation without making assumptions on the objects shapes [11]. The IWT combines automation and efficient interactive control in a coherent algorithm while completely avoiding oversegmentation which is the major problem of the classical WT. The use of Watershed transform is convincing as it always able to produce a complete division of the image. However, it always suffers from oversegmentation and sensitivity to false edges. Therefore, Watershed transform often needs a preprocessing to work well in the algorithm. To overcome the limitation, watershed transform is combined with K-means clustering to produce a primary segmentation of the image before being applied the watershed segmentation algorithm [12].

In this paper, nine sets of image data are experimented on the automated algorithm of watershed transforms in order to perform object segmentation. All of the scanned images are acquired from National Heart Institute of Malaysia. Datasets are obtained from the patients undergoing the TAVI procedure where all of image data consist of parasternal long axis view. At the first stage of the algorithm, the intensity of the input image is adjusted in order to

suppress the unwanted object and enhance the intensity of desired region. Then, histogram of the adjusted image is graphically analyzed. In the preprocessing, these method is applied to overcome a major limitation of this novel method itself which to avoid oversegmentation.

A normal distribution of the pixel value that usually represents a Gaussian shape is desired in order to obtain an optimal output once the input image enhanced. A good enhanced image denotes a better appearance of the image after processed. The image is then undergoing the watershed transform method in order to isolate the object and remove the unwanted region. The segmentation process is essentially based on the grayscale morphological operation. The aim of this paper is to perform a measurement on the aortic annulus. Therefore, once the desired object has been successfully segmented, an algorithm used to separate the AA and LVOT is performed. Hence, the intersection point between these two regions is marked and the distance corresponds to the diameter of aortic annulus.

## PROPOSED FRAMEWORK

There are three main parts of segmenting and measure the aortic annulus of the CT scan image. The first part is the image enhancement using median filter followed by the segmentation algorithm which is marker-controlled watershed transform. Two types of morphological operation which are image skeleton and intersection point have been applied to detect the aortic annulus. Finally, the size of annulus is obtained by measuring the distance between two points using Euclidean distance formula. Figure 2 shows the flow of proposed framework.

### Pre-Processing Stage

Image preprocessing is extremely essential to ensure the high accuracy of the following steps of the system as it is performed in the very beginning of the processing algorithm. The CT cardiac data images usually consist of artifacts that will affect the quality of captured images. The noise is typically due to motion beam hardening and metal artifact [13]. Thus, preprocessing procedure can be the medium of noise elimination to improve the quality and features in the image. The enhancement method can also be used to remove the film artifacts and filter the images whereby this method is used to improve the visual appearance of an image that eventually let it to form a new image that matches for analysis by human or machine [14]. Besides, contrast enhancements helps in improving the appearance of the objects in the image by enhancing the brightness so that the objects and their backgrounds can be differentiated. Typically, the use of gray-level histogram can be created from this enhancement method. It is done by counting the number of gray level value in each pixel occurred divided by the total number of pixels in the image to create a distribution of the percentage of each gray level.

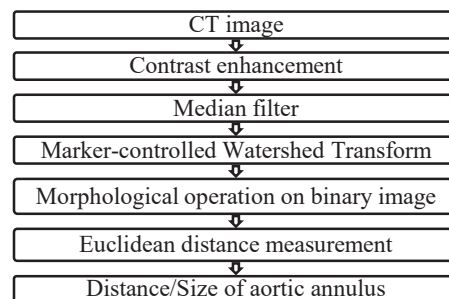


FIGURE 2. Steps of methodology

Median filtering, also known as nonlinear method used to remove noise from images. It is widely used as it is very effective at removing noise while preserving edges. It is particularly effective at removing ‘salt and pepper’ type noise. The median filter works by moving through the image pixel by pixel, replacing each value with the median value of neighbouring pixels. The kernel size of  $3 \times 3$  has been used in this analysis. Larger window sizes such as  $7 \times 7$  and  $9 \times 9$  may distort the image due to the high difference between the selected median pixel and the original pixel value. This median pixel which is mapped on the new image will produce a huge gap between neighborhood pixels which results in blurriness of the image. In [15], the performance of using several sizes of window have been studied. It shows that, median filter with kernel size of  $3 \times 3$  gives a higher power signal to noise ratio (PSNR) value compared to other window size when the noise is added into the image.

## Marker-Controlled Watershed Transform

A combination of erosion and dilation is part of the morphological operation where erosion operation is used to remove small object from a binary image while the dilation operation usually uses a structuring element for probing and expanding the shapes contained in the input image. The resulting output from those operations will be used as a marker to perform the watershed transform. These techniques will be beneficial in segmenting the accurate region as one of the limitations on watershed is often lead to the enlargement of the interest region. Therefore, marker computational will be an additional preprocessing of watershed transform to avoid over segmentation.

Figure 3 shows the sequent steps of creating the marker image. The first step is to compute the gradient image by using the image obtained from median filtering. Then, opening and closing image are computed followed by the image reconstruction. Opening image is the erosion followed by dilation while closing image is vice versa. For the reconstruction of opening image, it is used to restore the original shape of the object that remains after erosion while the reconstruction of opening-closing is to restore the remaining object after dilation.

Conversion of binary image before performing image erosion is necessary. Assumption of binary image,  $I(u, v)$  as the entire pixel located in the foreground can be stated as:

$$Q_I = \{(u, v) | I(u, v) = 1\} \quad (1)$$

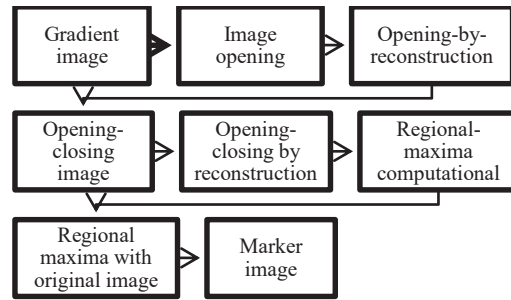


**FIGURE 3.** Steps of marker computational

Single variable for a coordinate pair can be written as,  $p = (u, v)$ . Hence,

$$Q_I = \{p | I(p) = 1\} \quad (2)$$

Dilation of an image  $I$ , by the structure element of  $H$  can be written as:

$$I \oplus H = \{(p + q) | p \in I, q \in H\} \quad (3)$$

A copy of structuring element,  $H_p$  is consolidated and place to the center of each of pixel location,  $p$  in foreground image. To simplify Equation (3), dilation can be written as:

$$I \oplus H = \bigcup_{p \in I} H_p \quad (4)$$

Erosion can be used to shrink off the foreground object where the erosion of an image,  $I$  by the structure element  $H$  is defined as:

$$I \ominus H = \{p \in Z^2 | (p + q) \in I, \text{ for every } q \in H\} \quad (5)$$

It can also be simplified as:

$$I \ominus H = \{p | H_p \subseteq I\} \quad (6)$$

where only pixel  $p \in I$  is kept so that  $H_p$  will fit inside image  $I$ . Implementation of erosion theory into the algorithm can be done by follow this operation,  $I \ominus H = \overline{(\overline{I} \oplus H^*)}$ . Inversion of image  $\overline{I}$  and structuring elements  $H$  are done to

obtain  $I'$  and  $H^*$  respectively. Next will be the dilation of  $I'$  with the reflected structure element,  $H^*$  is performed. Finally, the respective output is inverted to obtain eroded image. Opening operation is erosion followed by dilation, where it can be written as below.

$$I \bullet H = (I \ominus H) \oplus H \quad (7)$$

Stray foreground structures that are smaller than the  $H$  structure element will disappear. Larger structures will remain. Closing operation is a dilation followed by erosion. Therefore, holes in the foreground those are smaller than  $H$  will be filled. Closing operation can be written as below.

$$I \bullet H = (I \oplus H) \ominus H \quad (8)$$

Regional maxima are connected components of pixels with a constant intensity value,  $t$ , whose external boundary pixels all have a value less than  $t$ . In binary image, pixels that are set to 1 identify regional maxima while all other pixels are set to 0. Therefore, the resultant image from this morphological operation can be labeled as a marker to the Watershed method.

Direct application of gradient image on Watershed transformation may lead to the oversegmentation. Therefore, morphological operation consisting of structuring elements and reconstruction operators such erosion and dilation which has been discussed above are applied to mark the AA and LVOT efficiently. The combination of opening and closing images together with the reconstruction operator are used to clean up the image and remain the foreground objects as markers. These markers are extremely important because they help in modifying the gradient image obtained from Sobel filter and applying the arithmetic operation to the filtered image to compute the gradient magnitude so that the gradient of the edges is higher while the gradient inside the object is lower. Consequently, the borders of the object are well-shaped. In addition, minima imposition will modify the intensity of the image using morphological reconstruction to isolate the image so that it has only regional minima wherever greyscale image is nonzero.

Watershed transform is a convincing method for segmentation based on mathematical morphology [16]. As mentioned previously, direct implementation of the watershed transform towards the gradient image may lead to oversegmentation. Therefore, markers are the essential element to overcome the limitation of this powerful tool. We can consider the image as a landscape or topographic relief where the gray level of each pixel corresponds to a physical elevation. Immersing the landscape in a lake with holes pierced in local minima, catchment basins will fill up with water starting at these local minima. At points where water coming from different basins would meet, dams are built. This process ends when the water level has reached the highest peak in the landscape. As a result, the landscape is partitioned into regions or basins separated by dams, called watershed lines or simply watersheds [17]. Figure 4 shows the illustration of topographic relief of watershed tool.

## **Morphological Operation on Binary Image**

In this section, a method of skeletonizing the binary image followed by the extraction of branch point has been introduced. The distance of the intersection point that represents the diameter of aortic annulus is a crucial data to be input in the next following analysis. Thinning is a morphological operation used to remove selected foreground pixel just like erosion or opening resulting a minimum set of topology that preserving the original shape in that particular image [18]. Normally, thinning method is only applied to binary images and it will produce another binary image as output. An extensive studied on the methodologies of thinning operation for 2D binary images have been deeply discussed [19]. In this research, a method of thinning operation based on three vital conditions is adopted [18].

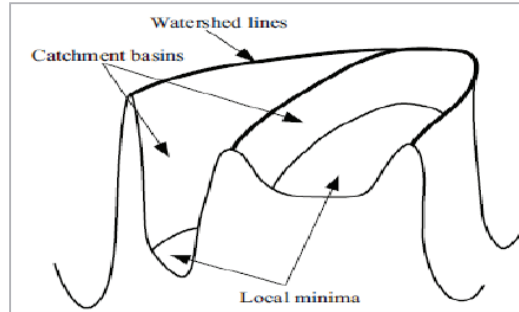


FIGURE 4. Topographic relief of watershed tool

Once the thinning process is done, the resulting output will be input to another morphological operation know as branch point where this operation will computed the intersection point of the skeleton image. If the certain pixel is surrounded by the adjacent and neighbor pixels, the algorithm will start the iteration to find the end point of each skeleton branch. Once end point of the branches is found, the iteration will be stopped immediately. The meeting point of those branches is selected as a branch point. Euclidean distance calculation is then being applied to measure the distance between those two points, where the result obtained in pixel and converted to millimeter so that comparison to real data can be made.

## RESULTS AND DISCUSSION

In pre-processing stage, contrast enhancement together with two types of filtering techniques have been applied to the input image for the purpose of enhancing the appearance and the quality as well as preserving and sharpening the edges of the ROI. Figure 5 (a) shows the raw image of CT scan imaging, while Fig. 5 (b) show the output obtained after the input data undergone the median filter. Aortic annulus in CT image has a higher brightness due to contrast agent inserted to the patient during the procedures. It is more presented compared to its background. Therefore, based on this characteristic of input image, a pre-processing method will produce a new image which preserves the ROI and suppresses the background components. The output is then used to the next analysis where the method used suited the data, which will produce accurate segmentation of analysis.



FIGURE 5. (a) Raw CT image and (b) image after median filtering

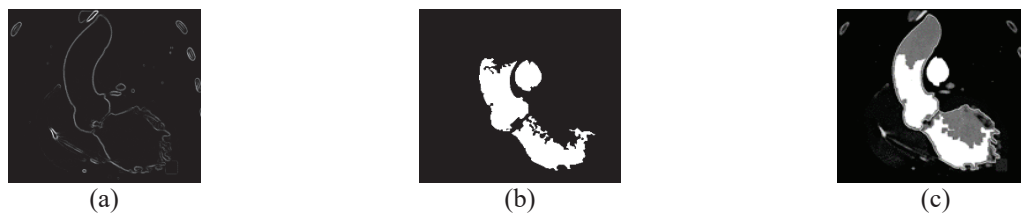
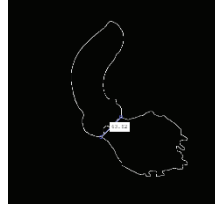


FIGURE 6. Output image after (a) gradient magnitude, b) regional maxima using opening-closing by reconstruction and (c) superimposed image of marker and object boundary



**FIGURE 7.** Conversion of watershed segmentation output of (a) label to RGB image and (b) RGB to greyscale image



**FIGURE 8.** Measurement of aortic annulus

Next analysis includes the detection of edges for the enhanced image that will assist in the formation of mask, where it is used as the reference image for the watershed segmentation method. The most common type of edge detection is used, known as gradient operator. Mathematically, the gradient magnitude,  $g(x, y)$  for an image function,  $f(x, y)$  is computed as:

$$g(x, y) \cong (\Delta x^2 + \Delta y^2)^{\frac{1}{2}} \quad (9)$$

where the convolution of the created mask with the image data can be made by aligning the mask with the  $x$  and  $y$  axes to compute the values of  $\Delta x$  and  $\Delta y$ .

Initially, a mask is created based on the Sobel operator where this method has been extensively used as it gives a decent delineation for detecting the edges. In this analysis, the mask of 3 by 3 neighborhood has been used. The marker used to perform the watershed segmentation is done using morphological operation where the combination of opening and closing images is applied to the filtered image where it is originally obtained by performing image filtration using median filters. Figure 6 shows the sequence output image obtained in order to compute the marker for watershed where (a) is the gradient magnitude image, (b) is the regional maxima of opening-closing by reconstruction where the new binary image is obtained and it shows the eroded region of aortic annulus where the image data is initially produced after filtering the input data while (c) is the superimposed marker and object boundary on the filtered image.

The preserved region shows the effect of opening and closing operation on filtered image based on selected structuring element where the higher pixel intensity is the only parameter that is taken into consideration. In this analysis, the type of structuring element used is 'disk'. Opening operator preserves foreground regions that have similar shape to the structuring element where initially foreground region in filtered image is brighter compared to its background. This can be seen in Fig. 5 (b).

However, as the sequential operation of opening and closing is performed, somewhat it leads to the generation of new unwanted object or region due to the effect of the closing operation. The normal morphological closing operation preserves the background regions that have a similar shape to its structuring element, while eliminating all other regions of background pixels. This can be seen in Fig. 6(b) where there is a circle region beside the ascending aorta which imitates the structuring element and it is undesirable and may distract the next analysis.

Next, the watershed segmentation based on marker image is done. The fundamental of this method is marker image acts as a local minimum in a catchment basin. Water will be filled in each of the local minima region. As both regions are full with water, the watershed line is produced. The marker image is used to avoid over segmentation as the function of local minima region is to act as a reference point which indicates the source of water in the catchment basin. Figure 6(c) shows the marker and object boundary superimposed on filtered image.

After the watershed transform, a global thresholding is applied to the segmented image. This requires an appointment of certain intensity value which is also known as threshold value. For instance, all voxels having intensity value below the threshold belong to one phase, and the remainder belongs to the other. Global thresholding produces

a better output and it is an unsophisticated segmentation choice. Before that a conversion of RGB to grayscale image is required. Figure 7(a) shows the coloured watershed label matrix, while Fig. 7(b) shows the output of global thresholding based on RGB image where the foreground objects represents two different intensities while the background is composed of uniform intensity. Lastly, the distance of aortic annulus is computed based on Euclidean distance. The intersection point between AA and LVOT indicates the actual distance of annulus. The previous output is first skeletonized before computing the branch points inside the region. Obtaining the distance between two points in pixel can be done through an automated measurement. The annulus distance can also be computed in millimeter by multiplying the value in pixel with 0.4 that indicates the resolution of CT scan modality. Figure 8 shows the measurement of annulus distance obtained in pixel.

For benchmarking purposes, we tested our data image on two different approaches, which belong to the same category of region-based segmentation method, but both are from different generation. The methods include region growing and deformable models. According to [20], they have made an intensive discussion on methods of segmenting the medical images. All methods are categorized into three generations where each generation enhances an additional level of algorithmic complexity to perform a better analysis. The first generation of medical image segmentation is composed of the simplest algorithm used for image analysis such as intensity threshold and region growing while second generation provides a deeper analysis and application of uncertainty models as well as methods for optimizing. Methods included in this generation are deformable models and graph search. Third generation was the advance method of segmentation the medical image where it is used to incorporate higher-level knowledge into segmentation process or extending the methods of previous generation to produce accurate segmentation in automated process where the methods that belong to this generation are shape models, appearance models, rule-based and coupled surfaces.

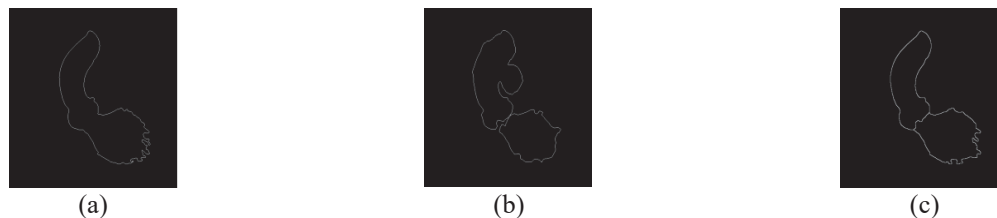


FIGURE 9. Images after annulus segmentation of (a) region growing, (b) deformable models and (c) proposed method

TABLE 1. Comparison of annulus sizing between manual marking and other methods

Method	Exact Annulus Sizing (mm)	Error
Manual marking	24.9	-
Region growing	23.6	1.3
Deformable models	27.7	2.8
<b>Proposed</b>	<b>25.1</b>	<b>0.2</b>

In this analysis, object segmentation is performed using the methods that have been discussed previously and for the purpose of comparing the accuracy of annulus sizing, the proposed method of measuring the aortic annulus size which uses combination of morphological operations is applied. Figure 9 shows the segmented ROI where each method apparently manages to preserve the outline of the object. However, there are some limitations that need to be addressed for this application. As the main intention of the proposed framework is to perform the automated object segmentation of medical images, this region growing method is not suitable to be used in order to perform the automatic analysis as this approach requires the selecting of an arbitrary seed pixel to start the operation. In Table 1, it shows that the proposed method produces the lowest error value which corresponds to the closest value of automated annulus sizing towards the manual sizing.

## CONCLUSION

The aim of this research is to perform an automated measurement of annulus sizing that is highly accurate. This can decrease the workload of cardiologists before performing the TAVI procedures. The correct measurement of aortic annulus size is important as the measurement is used for selecting the best size of prosthetic valve for TAVI patients. Inaccurate deployment of prosthetic valve would pose risks to the patients. The advanced use of image processing technique in determining the optimal size of aortic annulus using an automated segmentation gives promising results.

In the proposed framework, in preprocessing stage, a contrast enhancement followed by the median filtering have been used to enhance the foreground objects in the image. Then, watershed segmentation method is applied to the image data as the topological gradient provides a global analysis of the image. Since watershed transform usually suffers from oversegmentation, an introduction of marker that can control the segmentation of watershed is made to overcome this limitation. From the experimental results, the usual segmentation problem which always appear on the watershed transformation is solved by applying the marker in order to control the segmentation process. Hence, watershed transform produces a successful segmentation of ROI. Once the segmented regions are obtained, the measurement of annulus is done using morphological operation that includes the image skeletonize and detecting the branch points. The result obtained in pixel is then converted to mm for better presentation. As all the input images acquired are from patients that have undergone the TAVI procedure, it is beneficial to validate the results obtained from the analysis where the comparison between automated measurement and ground truth can be made. Furthermore, the advantages of the proposed methods are the production of fast computation and accurate annulus size measurement as well as production of good image segmentation that leads to the accurate annulus size measurement.

## ACKNOWLEDGMENTS

The research was made possible by the funding of the Ministry of Higher Education (MOHE) Malaysia and Universiti Teknologi Malaysia (UTM) under the Research University Tier 1 Grant (vote 12H72).

## REFERENCES

1. A. Zajarias and A. G. Cribier, *Journal of the American College of Cardiology* **53**, 1829-1836 (2009).
2. C. Tamburino, D. Capodanno, A. Ramondo, A. S. Petronio, F. Etti, G. Santoro, S. Klugmann, F. Bedogni, F. Maisano, A. Marzocchi and A. Poli, *Circulation* **123**, 299-308 (2011).
3. T. Arai and T. Lefèvre, *Journal of Cardiology* **63**, 178-181 (2014).
4. J. J. Bax, V. Delgado, V. Bapat, H. Baumgartner, J. P. Collet, R. Erbel, C. Hamm, A. P. Kappetein, J. Leipsic, M. B. Leon and P. MacCarthy, *European Heart Journal* **35**, 2627-2638 (2014).
5. N. Piazza, R. Lange, G. Martucci and P. W. Serruys, *Archives of Cardio Diseases* **105**, 165-173 (2012).
6. W. Khan, *Journal of Image and Graphics* **1**, 166-170 (2014).
7. N. R. Pal and S. K. Pal, *Pattern Recognition* **26**, 1277-1294 (1993).
8. C. Jia-xin and L. Sen, "A medical image segmentation method based on watershed transform," in IEEE 5th International Conference on Computer and Information Technology, edited by N. Gu *et al.* (Institute of Electrical and Electronics Engineers, Piscataway, NJ, 2015), pp. 634-638.
9. J. B. Roerdink and A. Meijster, *Fundamenta Informaticae* **41**, 187-228 (2000).
10. V. Grau, A. U. J. Mewes, M. Alcaniz, R. Kikinis and S. K. Warfield, *IEEE Transactions on Medical Imaging* **23**, 447-458 (2004).
11. H. K. Hahn and H. O. Peitgen, "IWT-interactive watershed transform: A hierarchical method for efficient interactive and automated segmentation of multidimensional gray-scale images," in Proceedings of SPIE 5032, (Society of Photo-Optical Instrumentation Engineers, Bellingham, WA, 2003), pp. 1-11.
12. H. P. Ng, S. H. Ong, K. W. C. Foong, P. S. Goh and W. L. Nowinski, "Medical image segmentation using k-means clustering and improved watershed algorithm," in IEEE Southwest Symposium on Image Analysis and Interpretation (Institute of Electrical and Electronics Engineers, Piscataway, NJ, 2006), pp. 61-65.
13. G. Hamarneh and X. Li, *Image and Vision Computing* **27**, 59-68 (2009).
14. J. F. Barrett and N. Keat, *Radiographics* **24**, 1679-1691 (2004).
15. E. S. A. Ahmed, R. E. Elatif and Z. T. Alser, *International Journal of Signal Processing, Image Processing and Pattern Recognition* **8**, 343-352 (2015).
16. N. Shameena and R. Jabbar, *International Journal of Engineering Research and Technology* **3**, 336-341 (2014).
17. F. Meyer and S. Beucher, *Journal of Visual Communication and Image Representation* **1**, 21-46 (1990).
18. R. M. Habibur and M. R. Islam, *AIUB Journal of Science and Engineering* **12**, 105-116 (2013).
19. H. Xia and P. G. Tucker, "Distance solutions for medial axis transform," in 18th International Meshing Roundtable, edited by B. W. Clark (Springer, Berlin, Heidelberg, 2009), pp. 247-265.
20. D. J. Withey and Z. J. Koles, "Medical image segmentation: Methods and software," in IEEE Joint Meeting of the 6th International Symposium on Noninvasive Functional Source Imaging of the Brain and Heart and the International Conference on Functional Biomedical Imaging (Institute of Electrical and Electronics Engineers, Piscataway, NJ, 2007), pp. 140-143.